AIP | Journal of Applied Physics

Correlation between nanoparticle and plasma parameters with particle growth in dusty plasmas

Kil Byoung Chai, C. R. Seon, C. W. Chung, N. S. Yoon, and Wonho Choe

Citation: J. Appl. Phys. **109**, 013312 (2011); doi: 10.1063/1.3531546
View online: http://dx.doi.org/10.1063/1.3531546
View Table of Contents: http://jap.aip.org/resource/1/JAPIAU/v109/i1
Published by the American Institute of Physics.

Correlation between nanoparticle and plasma parameters with particle growth in dusty plasmas

Kil Byoung Chai,[1] C. R. Seon,[1,a)] C. W. Chung,[2] N. S. Yoon,[3] and Wonho Choe[1,b)]
[1]*Department of Physics, Korea Advanced Institute of Science and Technology, 335 Gwahangno, Yuseong-gu, Daejeon 305-701, Republic of Korea*
[2]*Department of Electric and Computer Engineering, Hanyang University, 17 Haengdang-dong, Seongdong-gu, Seoul 133-791, Republic of Korea*
[3]*Department of Electrical Engineering, Chungbuk National University, 48 Gaesin-dong, Heungdeok-gu, Cheongju, Chungbuk 361-763, Republic of Korea*

(Received 20 September 2010; accepted 25 November 2010; published online 14 January 2011)

Since plasma parameters are altered by dust particles, studying how plasma parameters are related to dust particle growth is an important research issue in dusty plasma. In this paper, the correlation between plasma parameters (electron temperature and ion flux) and particle parameters (particle radius and density) is investigated in silane plasma both experimentally using a floating probe and theoretically by solving balance equations including an additional electron and ion loss to the dust. The results reveal that while the ion flux shows two peak values in the early discharge phase and at the end of coagulation phase, the electron temperature shows a sudden increase in the coagulation step and a gradual decrease in the molecular accretion step. Moreover, the calculated results with the secondary electron emission taken into account produce the best fit with the experimental results. Thus the study confirms that the secondary electron emission plays a crucial role in the coagulation of the dust particles. © *2011 American Institute of Physics*. [doi:10.1063/1.3531546]

I. INTRODUCTION

Dusty plasmas are of considerable interest in various fields of science and technology. In astrophysics, dusty plasmas have been intensively studied because they are ubiquitous in space, including interstellar clouds, nova ejecta, and planetary magnetospheres.[1] In industrial plasma processes, the generation, growth, and transport of dust particles have been investigated in efforts to remove them because they are responsible for reducing production yield and reliability in plasma enhanced chemical vapor deposition and reactive ion etching.[2] With respect to high temperature plasma, the dust generated by plasma–wall interactions in fusion devices is regarded as a safety hazard, and this issue has become an important area of research.[3] Recently, it has been shown that the optical and electrical properties of photovoltaics are enhanced by plasma-aided nanoparticle synthesis.[4]

In most dusty plasmas, dust particles are spontaneously generated by chemical reactions between radicals or plasma–wall interactions and grow inside the plasma. Moreover, it has been reported that plasma parameters such as electron temperature and ion density are altered by dust generation.[5] It is, therefore, inevitable to investigate how plasma parameters are correlated with dust particle growth, an issue that may be essential for more efficiently controlling and using dusty plasmas. However, making accurate measurements of various plasma parameters in dusty plasmas is generally a nontrivial process. For instance, although Langmuir probes are widely used in low temperature plasmas, the conventional Langmuir probes may fail to provide accurate information due to probe tip contamination caused by chemical reactions occurring inside the plasma. Furthermore, while electron density can be measured by a microwave interferometer, electron temperature cannot. In this work, we simultaneously obtained electron temperature and ion flux in silane dusty plasmas using a recently developed floating-type probe.[6] Since the probe employs a tens of kilohertz sinusoidal waveform bias voltage and measures ac current rather than dc current, it is little affected by deposition on the probe tip as long as the deposition thickness is not too large.

The goal of this work is to investigate the behavior of the electron temperature and ion flux with dust particle growth. To achieve this, the dust particle size and density are measured by transmission electron microscopy (TEM) and the laser extinction method. The measured electron temperature and ion flux are compared with the values calculated by solving particle and power balance equations including the electron and ion loss to the dust particles. The findings from our work demonstrate that it is possible to predict how the plasma parameters change with the dust generation and growth and it is possible to predict dust size and growth by measuring the plasma parameters.

II. EXPERIMENTAL SETUP

Figure 1 is a schematic of the experimental setup where a typical capacitively-coupled type plasma source is depicted. The circular electrode of 6 cm in radius placed at the bottom of the cylindrical reactor chamber of 13 cm in radius and 18 cm in height was powered by a 13.56 MHz radio frequency (rf) power supply (RFPP RF10S) via an automatic impedance matcher (RFPP AMNPS-2A). The plasma was produced by supplying a silane diluted argon gas consisting of 5% SiH_4 and 95% Ar.

a)Present address: National Fusion Research Institute, 113 Gwahangno, Yuseong-gu, Daejeon 305-333 Korea.
b)Electronic mail: wonhochoe@kaist.ac.kr.

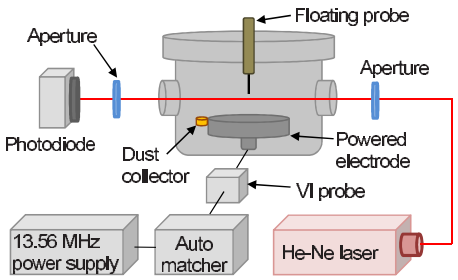

FIG. 1. (Color online) A schematic of the experimental setup.

In order to measure the plasma parameters, a floating-type probe[6] was used where a 50 kHz sinusoidal waveform voltage was applied to the probe tip and the ac current was collected. The dimension of the probe tip was 1 mm in diameter and 10 mm in length with the basically same structure as an ordinary single Langmuir probe. Electron temperature and ion flux were determined by the linear and nonlinear responses of the ac current rather than the dc current. The probe measurement was carried out in the bulk plasma region at 5 cm vertically above the electrode to minimize the plasma perturbation. The sheath thickness estimated by the plasma emission image was less than 1 cm. The difference in the laser scattering intensities due to the presence of the probe and the biasing of the probe at the measurement location showed less than 15% difference, indicating that the perturbation in the dust particles caused by the probe is relatively inconsiderable. A typical TEM grid was placed at the bottom of the chamber to collect the generated dust particles, and their sizes were obtained by analyzing the TEM (Technai T30) photographs. The dust number density was measured by the laser extinction method in which the number density was determined by the intensity ratio of the original and the transmitted laser beams through the distributed particles inside the plasma (Fig. 1). The details of the measurement are described in our previous report.[7]

In addition, the driven voltage and the passing current through the electrode and the phase difference between them were measured by a conventional V-I probe that was positioned between the matching box and the electrode, as depicted in Fig. 1.

III. EXPERIMENTAL RESULTS

The solid curves shown in Fig. 2 demonstrate the temporal evolution of the measured electron temperature T_e and ion flux Γ_i at 34 mTorr pressure and 50 W rf power, which is brought about by the generation and growth of dust particles inside the plasma. It is seen that T_e first increases sharply from 2 to 6 eV in 0–100 s and thereafter decreases slowly to 4.5 eV. On the other hand, Γ_i shows two peaks at 5 and at 80 s. Such electron temperature behavior of first increasing and later decreasing was commonly observed in other operation conditions.

The time evolution of the particle radius r_p and density n_p is presented in Fig. 3. The nonlinear growth is shown in the first 50–100 s which is followed by linear growth during 100–200 s while n_p gradually decreases during 0–200 s. As per generally known three growth steps of dust particles in

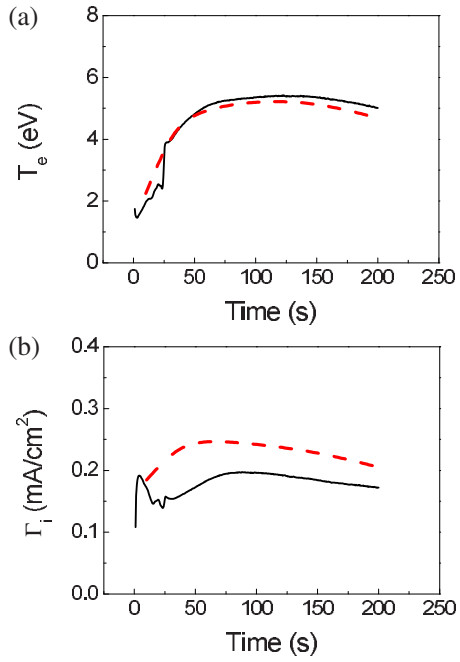

FIG. 2. (Color online) Time evolution of (a) electron temperature T_e and (b) ion flux Γ_i. The solid and dashed curves, representing the measured values and the modeling results, respectively, show reasonable agreement.

silane plasmas,[8] the nucleation step occurred right after the plasma ignition and then it was followed by the coagulation growth step that matches with the nonlinear growth. Finally, the molecular accretion growth step, which corresponds to the linear growth, starts from 100 s. These three growth steps are consistent with findings of previous works.[7–9]

The temporal behavior of applied voltage and the rf power delivered to the plasma is shown in Fig. 4. While the driven voltage only slightly changes (<2%), the delivered rf

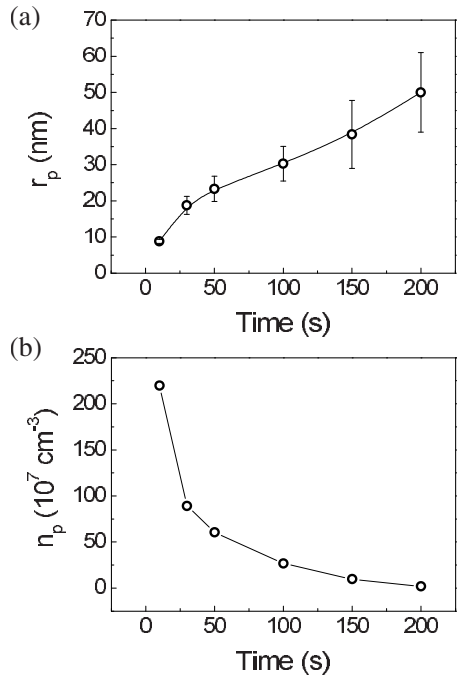

FIG. 3. (Color online) Time evolution of (a) the measured dust particle radius r_p, and (b) number density n_p.

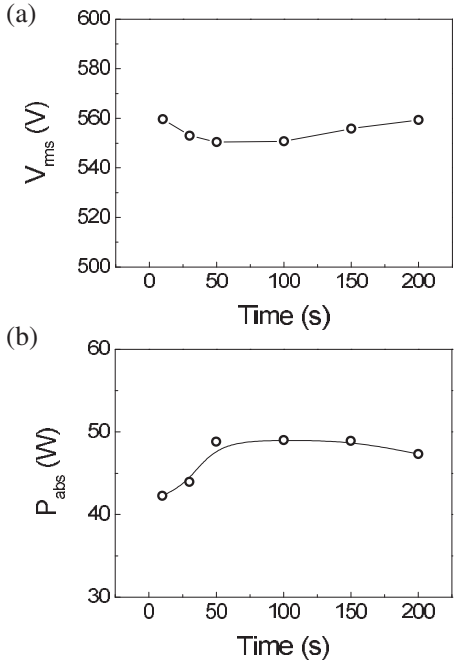

FIG. 4. (a) Voltage at the electrode and (b) delivered rf power measured by a V-I probe as a function of time.

power varies quite a lot (~15%). Moreover, both the driven voltage and the delivered power are at a minimum and a maximum at around 50 s to 100 s, respectively, which corresponds to the end of the coagulation step. Therefore, it is suggested that the plasma impedance varies with time, i.e., in accordance with dust growth.

IV. DISCUSSION

We performed modeling in an effort to understand the electron temperature T_e and ion flux Γ_i changes by solving the following equations. The particle balance equation, including the electron and ion loss toward the dust particles, is given by[10]

$$\sum_s n_{i,s}\left[A_{\text{eff}}u_{B,s}+S_{\text{ptl}}v_{i,s}\left(1-\frac{e\phi_p}{kT_{i,s}}\right)\right] = \sum_s \sigma_{0,s}v_e\left(1+\frac{2kT_e}{\varepsilon_{iz,s}}\right)\exp\left[\frac{-\varepsilon_{iz,s}}{kT_e}\right]n_{g,s}n_eV, \quad (1)$$

where $n_{i,s}$, $T_{i,s}$, $u_{B,s}$, $v_{i,s}$, and $\varepsilon_{iz,s}$ are the ion density, the ion temperature, the Bohm velocity, the ion thermal speed, and the ionization energy of s species, respectively; n_e, T_e, and v_e are the density, the temperature, and the thermal speed of electrons, respectively; A_{eff} and V are the effective plasma area and the plasma volume, respectively; ϕ_p is the floating potential of the dust particle, k is the Boltzmann constant, $\sigma_{0s}=\pi(e/4\pi\varepsilon_0\varepsilon_{iz,s})^2$, and $n_{g,s}$ is the neutral gas density of s species. In this work, s species denotes Ar or SiH_4, and only Ar^+ and SiH_3^+ ions are considered because they are the most likely formed species.[11] Here, $A_{\text{eff}}=2\pi R(Rh_L+Lh_R)$, where R and L are the radius and the height of the chamber, $h_L=0.86(3+L/2\lambda_i)^{-1/2}$, $h_R=0.80(4+R/\lambda_i)^{-1/2}$, and λ_i is the ion mean free path, respectively.[10] The first and the second terms on the left hand side of Eq. (1) describe the total particle loss to the surface of the plasma sheath and the dust particles, respectively. The right hand side of the equation represents the total volume ionization by electron-neutral collisions.

The power balance equation, including loss to the dust particles, is given by[10]

$$P_{\text{abs}}=\sum_s\left[en_{i,s}u_{B,s}A_{\text{eff}}(\varepsilon_{c,s}+\varepsilon_e+\varepsilon_i) + en_{i,s}v_{i,s}\left(1-\frac{e\phi_p}{kT_{i,s}}\right)S_{\text{ptl}}(\varepsilon_{c,s}+\varepsilon_{e,p}+\varepsilon_{i,p})\right], \quad (2)$$

where $\varepsilon_{c,s}$ is the collisional energy loss for s species, ε_e is the mean kinetic energy per electron lost ($=2.5kT_e$), ε_i is the mean kinetic energy per ion lost ($=0.8V_{\text{rf}}$ in the capacitively-coupled plasma where V_{rf} is the voltage driven at the electrode), $\varepsilon_{e,p}$ and $\varepsilon_{i,p}$ are the mean kinetic energy losses per electron and ion to the dust particle, respectively. The collisional energy loss of each species is calculated from the relation $K_{iz,s}\varepsilon_{c,s}=K_{iz,s}\varepsilon_{iz,s}+K_{ex,s}\varepsilon_{ex,s}+K_{el,s}(3m_e/M_s)kT_e$ where $K_{iz,s}$, $K_{ex,s}$, and $K_{el,s}$ are the ionization, excitation, and elastic collision rate constants of s species, respectively; $\varepsilon_{ex,s}$ is the excitation threshold energy of s species, and M_s is the atomic/molecular mass of s species. In this work, the rate constants for Ar were obtained from Ref. 10 and those for SiH_4 were obtained from Ref. 5. Note that we assumed $\varepsilon_{e,p}=2.5kT_e$, and $\varepsilon_{i,p}=0.5kT_e-e\phi_p$ because the ions gain and lose energy by $-e\phi_p$ in the presence of $0.5kT_e$ plasma potential. Here, the first and the second terms on the right hand side of Eq. (2) are the power dissipated to the surface A_{eff} by the ion outflow and the power absorbed by the dust particles, respectively.

Furthermore, the charge neutrality condition $n_e-Z_pn_p=\Sigma_s n_{i,s}$ is solved to obtain n_e, where the charge number of the dust particle is given by $Z_p=4\pi\varepsilon_0 r_p\phi_p/e$. Note that the relation $n_e=\Sigma_s n_{i,s}$ is no longer valid in dusty plasma due to the presence of negatively charged dust particles.

In addition to the particle and power balance equations and the charge neutrality condition, the dust charging equation should be solved to obtain ϕ_p. The ion and electron currents to the dust particles are given by[12]

$$I_i=\sum_s 4\pi r_p^2n_{i,s}e\left(\frac{8kT_{i,s}}{\pi m_{i,s}}\right)\left(1-\frac{e\phi_p}{kT_{i,s}}\right), \quad (3)$$

$$I_e=4\pi r_p^2n_ee\left(\frac{8kT_e}{\pi m_e}\right)\exp\left[\frac{e\phi_p}{kT_e}\right], \quad (4)$$

respectively, where m_e is the electron mass and $m_{i,s}$ is the ion mass of s species. Moreover, if the dust particle size is less than a few tens of nanometers, the secondary electron emission by electron impact can no longer be ignored.[13] Therefore, in this work, secondary electron emission is considered and its current to the dust is given by[13]

$$I_{see}=3.7I_e\delta_mF_5(E_m/4kT_e), \quad (5)$$

where δ_m is the peak yield for secondary electron emission, E_m is the impact energy for the peak yield, and $F_5(x)=x^2\int_0^\infty t^5\exp[-(xt^2+t)]dt$. Note that δ_m and E_m depend on the particle size and particle material and were taken from Ref.

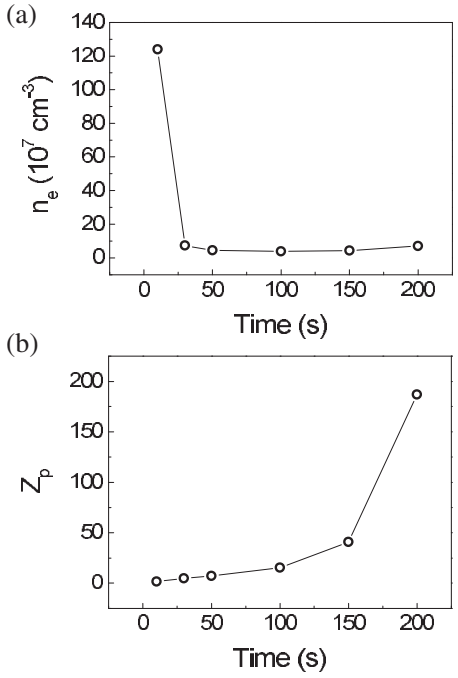

FIG. 5. (a) Calculated electron density and (b) dust charge number as a function of time.

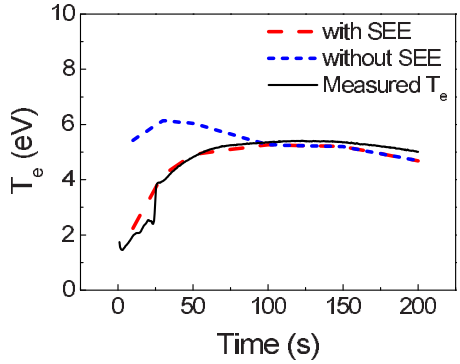

FIG. 6. (Color online) Calculated electron temperature with (dashed) and without (dotted) consideration of secondary electron emission from the dust. The solid curve denotes the measured value.

12. The dust potential ϕ_p was obtained from the fact that the total current to the dust particle becomes zero ($I_i - I_e + I_{see} = 0$) in a steady-state.

Now, the calculation procedure is described as follows. Using the measured values of r_p and n_p as the input parameter, T_e is calculated by Eq. (1) with $R=0.15$ m, $L=0.2$ m, $T_{i,\mathrm{Ar}}=T_{i,\mathrm{SiH_4}}=1/40$ eV, $n_{g,\mathrm{Ar}}=1.03\times10^{21}$ m^{-3} (34 mTorr $\times 0.95$), $n_{g,\mathrm{SiH_4}}=5.44\times10^{19}$ m^{-3} (34 mTorr $\times 0.05$), $\varepsilon_{\mathrm{iz,Ar}}=15.8$ eV, $\varepsilon_{\mathrm{iz,SiH_4}}=11.6$ eV, and $n_e/\Sigma n_{i,s}=1$, $\phi_p=0$ as an initial estimation. Then, $n_{i,\mathrm{Ar}}$, $n_{i,\mathrm{SiH_4}}$ are obtained using Eq. (2) with the measured V_{rf} and P_{abs} (time evolutions of V_{rf} and P_{abs} are considered). Then, n_e and ϕ_p are solved by the charge neutrality condition and Eqs. (3)–(5). Finally, T_e and Γ_i are obtained accurately by iterative calculations performed until $n_e/\Sigma n_{i,s}$ becomes saturated (until its stepwise change becomes less than 10^{-3} in this work).

Shown in Fig. 2 as dashed curves are T_e and Γ_i calculated in this manner. It is noted that the calculated T_e and Γ_i are in good agreement with those of the measured values, indicating that the dust particles serve as an additional loss channel for electrons and ions.

The calculated n_e and Z_p are described in Fig. 5. Notice that while n_e decreases drastically to about 1/10 of the total ion density, Z_p increases slightly but by less than 10 electron charges in the coagulation growth step. The result is explained as follows. In the beginning of the coagulation growth step, the average dust charge $eZ_p \approx -e$ due to secondary electron emission from the dust by high energy electron impact. If the secondary electron emission is ignored, Z_p becomes more negative and the coagulation growth becomes hindered. As the dust particle grows in size, I_{see}/I_e decreases due to the fact that the electron escape probability from the dust surface decreases.[12] Therefore, Z_p increases, and the amount of electrons captured by the dust increases. Consequently, n_e decreases drastically, and T_e increases sharply to compensate for the electron loss, as seen in Fig. 2(a).

Since n_e is very low after the coagulation growth step, dust particles now become the major charge carriers rather than electrons. Therefore, the plasma becomes more resistive due to the large dust mass compared to the electron mass. Consequently, the rf power transfer to the plasma becomes more efficient, and the ion flux is at its maximum at the end of the coagulation step. This phenomenon called α-γ' transition is reported in the previous work.[14]

As the dust size becomes larger than 30 nm, the secondary electron emission becomes no longer effective as described in Ref. 12. Therefore, Z_p increases significantly as presented in Fig. 5(b), meaning that a large repulsive electrostatic force is exerted between the dust particles, and the coagulation process cannot continue any more. Instead, the molecular accretion process involving SiH_3 and SiH_2 occurs. In the molecular accretion step, T_e decreases gradually in accordance with the total surface area of the dust particles.

Figure 6 shows the calculated T_e with (dashed) and without (dotted) taking secondary electron emission into account. As seen in the figure, the modeling result including secondary electron emission is in excellent agreement with the measurement, which means that secondary electron emission is crucial in the coagulation step of dust particles.

It is noted that negative ions such as SiH_3^- and SiH_2^- were not taken into account in our analysis. If negative ions are taken into account, the followings should be modified: first, recombination of negative and positive ions should be included in Eq. (1). Second, additional collisional energy loss should be added in $\varepsilon_{\mathrm{c,SiH_4}}$ of Eq. (2). Third, negative ion density should be included in the charge neutrality equation. On the other hand, the current of negative ions toward the dust particle can be neglected because negative ions do not have enough kinetic energy to overcome the negative floating potential of the dust particle. Consequently, the followings are expected in the modified analysis: first, decrease of electron density due to the negative ion density term in the charge neutrality equation; second, decrease of dust particle potential due to the electron density decrease; third, increase of electron temperature due to the additional loss term (recombination term) in Eq. (1); and finally, decrease of ion flux because of the increase of collisional energy loss $\varepsilon_{\mathrm{c,SiH_4}}$ in

Eq. (2). The most important issue here is how many negative ions are produced. The ratio of negative ion density to electron density was estimated for our experimental condition using the rate constants for positive SiH_3^+ ions and negative SiH_3^- ions given in Ref. 10. The calculation revealed that the ratio of negative ion density to electron density is smaller than 20%, and thus, T_e and Γ_i were recalculated including the negative ion density in the charge neutrality based on the density ratio. The results showed that the calculated T_e and Γ_i with and without negative ions are not significantly different, which indicates that the negative ion effect can be neglected for our discharge condition.

V. SUMMARY

Temporal behavior of electron temperature and ion flux was investigated by modeling and measurement in silane plasma with dust growth. Interestingly, the electron temperature and ion flux changed with time in accordance with the three well known dust growth steps. In order to understand the underlying physics, we solved particle and power balance equations including the electron and ion losses to the dust particles. The balance equation of the current to the dust was also solved including secondary electron emission from the dust by electron impact. The result demonstrates that the calculated electron temperature and ion flux are in good agreement with the measurements, suggesting that dust particles act as a loss channel of the electrons and ions. Moreover, the electron temperature increases sharply in the coagulation step and gradually decrease in the molecular accretion step. The ion flux has two maximum values at the early discharge phase (i.e., in the nucleation step) and at the end of the coagulation step due to the fact that the plasma becomes more resistive. These results suggest that it is possible to predict dust parameters (i.e., dust growth step and size) by measuring the plasma parameters (i.e., electron temperature and ion flux).

ACKNOWLEDGMENTS

This research was supported by National R&D Program through the National Research Foundation of Korea (NRF) funded by the Ministry of Education, Science, and Technology (Grant No. 2010-0020037).

[1]C. K. Goertz, Rev. Geophys. **27**, 271 (1989).
[2]H. H. Hwang and M. J. Kushner, Appl. Phys. Lett. **68**, 3716 (1996).
[3]J. Winter and G. Gebauer, J. Nucl. Mater. **266–269**, 228 (1999).
[4]M. Shiratani, K. Koga, S. Ando, T. Inoue, Y. Watanabe, S. Nunomura, and M. Kondo, Surf. Coat. Technol. **201**, 5468 (2007).
[5]I. Denysenko, K. Ostrikov, S. Xu, M. Y. Yu, and C. H. Diong, J. Appl. Phys. **94**, 6097 (2003).
[6]M. H. Lee, S. H. Jang, and C. W. Chung, J. Appl. Phys. **101**, 033305 (2007).
[7]C. R. Seon, H. Y. Park, W. Choe, S. Park, and Y. H. Shin, Appl. Phys. Lett. **91**, 251502 (2007).
[8]A. Bouchoule and L. Boufendi, Plasma Sources Sci. Technol. **2**, 204 (1993).
[9]C. Hollenstein, J. L. Dorier, J. Dutta, L. Sansonnens, and A. A. Howling, Plasma Sources Sci. Technol. **3**, 278 (1994).
[10]M. A. Lieberman and A. J. Lichtenberg, *Principles of Plasma Discharges and Materials Processing* (Wiley, New York, 1994).
[11]K. De Bleecker, A. Bogaerts, R. Gijbels, and W. Goedheer, Phys. Rev. E **69**, 056409 (2004).
[12]A. Bouchoule, *Dusty Plasmas: Physics, Chemistry and Technological Impact in Plasma Processing* (Wiley, New York, 1999).
[13]J. Goree, Plasma Sources Sci. Technol. **3**, 400 (1994).
[14]J. Perrin, C. Bohm, R. Etemadi, and A. Lloret, Plasma Sources Sci. Technol. **3**, 252 (1994).